Nuclear Instruments and Methods in Physics Research A 836 (2016) 105–112

Contents lists available at ScienceDirect

Nuclear Instruments and Methods in Physics Research A

journal homepage: www.elsevier.com/locate/nima

Detector production for the R3B Si-tracker

M. Borri [b,*], R. Lemmon [a], J. Thornhill [b], R. Bate [b], M. Chartier [b], N. Clague [a], R.-D. Herzberg [b], M. Labiche [a], S. Lindsay [b], P. Nolan [b], F. Pearce [b], W. Powell [b], D. Wells [b]

[a] STFC Daresbury Laboratory, Daresbury, Warrington WA4 4 CE, UK
[b] University of Liverpool, Department of Physics, Oxford Street, Liverpool L69 7ZE, UK

ARTICLE INFO

Article history:
Received 29 May 2016
Received in revised form
22 August 2016
Accepted 23 August 2016
Available online 24 August 2016

Keywords:
Silicon strip detectors
Charged particle tracking
Radioactive ion beams
Detector production

ABSTRACT

R3B is a fixed target experiment which will study reactions with relativistic radioactive beams at FAIR. Its Si-tracker will surround the target volume and it will detect light charged-particles like protons.

The detector technology in use consists of double-sided silicon strip sensors wire bonded to the custom made R3B-ASIC.

The tracker allows for a maximum of two outer layers and one inner layer. This paper reports on the production of detectors necessary to build the minimum tracking configuration: one inner layer and one outer layer.

1. Introduction

FAIR [1] (Facility for Antiproton and Ion Research) is an accelerator complex under construction in Darmstadt, Germany. It will provide ion beams for a series of different and parallel experimental programs. NUSTAR [2] (NUclear STructure Astrophysics and Reactions) is one of the several collaborations exploiting the physics opportunities of such beams. Its scientific program aims at probing nuclear structure and to understand the origin of the elements in the universe. These studies will be performed with secondary beams of highly unstable nuclei. Secondary beams are produced by impinging primary ion beams on a production target. Ions break-up into other nuclei (highly unstable) and are separated in-flight within hundreds of ns by the magnetic spectrometer called SUPER-FRS [3] (SUPERconducting FRagment Separator).

R3B [4] (Reactions with Radioactive Relativistic Beams) is part of the NUSTAR scientific program. It is an experiment located at the focal plane of the high-energy branch of the SUPER-FRS. It allows for kinematically complete measurements of reactions with radioactive beams with unprecedented accuracy. The set-up capitalizes on the highest possible transmission of secondary beams (20Tm magnetic rigidity) provided by the SUPER-FRS.

2. R3B Si tracker

The R3B Si-tracker is shown in Fig. 1. A maximum of three layers can be installed in the vacuum vessel at the same time: one inner and two identical outers. A total of 30 detectors compose the three layers: 6 in the inner layer and 12 in each of the two outer layers. This equates to a total sensitive area of ~0.56 m^2 and 116,736 front-end channels. The angular coverage of the Si-tracker is 6–103°. Angles are measured from the forward direction of the beam axis using the nominal target position as the angle vertex.

The R3B Si-tracker detects light charged-particles, like protons, recoiling from the target volume. It has tracking and vertexing capabilities, and provides the possibility of performing multiplicity and energy measurements.

The capability of tracking recoils makes the Si-tracker a key instrument to study reactions like (p,2p). It measures the trajectories of recoiling protons and combines them to find the primary vertex. The tracking information is in turn merged with data from other sub-detector systems to reconstruct the reaction kinematics. The angular resolution of a computed trajectory is an important parameter for the precision of these measurements. It was considered to optimise layer position, sensor thickness and sensor granularity during design. It is expected that the angular resolution will not be limited by the intrinsic accuracy of the Si-tracker. For this purpose, simulations were employed to evaluate the angular resolution of high energy protons like those produced in a (p,2p) reaction. High energy protons of 250 MeV were emitted at an angle of 10° and generated at the centre of a CH_2 target. The

* Corresponding author.
E-mail address: marcello.borri@liverpool.ac.uk (M. Borri).

http://dx.doi.org/10.1016/j.nima.2016.08.050
0168-9002/

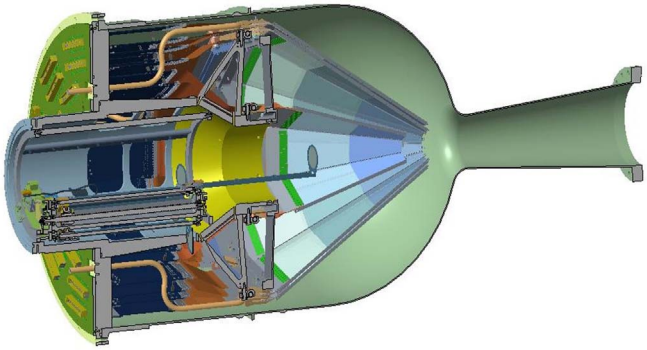

Fig. 1. The R3B Si-tracker mounted in the vacuum chamber with the target disk in the in-beam position. The tracker is portrayed in its extended configuration, consisting of one inner layer and two identical outer layers.

chosen energy is the upper limit of the energy range (50–250 MeV) for the recoiling protons of interest. An angle of 10° is a typical angle of emission for these high energy protons. The Si-tracker was simulated in the so-called extended configuration (1 inner and 2 outer layers). Two type of CH_2 targets were simulated. A thick target of 0.5 g/cm^2 and a thin target of 0.01 g/cm^2. The angular resolution was estimated to be 0.179° and 0.0336° respectively. Simulations show that scattering of recoils inside the target is a dominant factor in degrading angular resolution.

The R3B Si-tracker is operated in a moderately low radiation environment. The detector is expected to stand a total of 5×10^{10} particles per year. This value is much lower than that of a vertex detector in one of the LHC experiments. In that case a typical value of 10^{14}–10^{15} charged particles per year [5] is expected. Nonetheless, particular attention was paid during design to the position of the ASICs in the set-up. The conical configuration of the tracker minimizes the ASIC exposure to ionizing radiation. This is because recoils are mainly emitted at forward angles.

The Si-tracker will be operated in vacuum (~10^{-8} bar). The vacuum chamber containing the detector has a volume of ~0.148 m^3. It is made of aluminium and has walls ~2 mm thick.

Detectors in the vacuum chamber are supported by an aluminium structure and cooled. The cooling system is based on copper pipes and blocks, and it uses a mixture of water and glycol as coolant. The aim is to operate the detectors at a temperature of ~20°C.

Detectors are made of double sided strip sensor wire bonded to the custom made R3B-ASIC. Two different types of detectors are used: the inner layer detector and the outer layer detector. They are shown in Fig. 2. The inner layer detector is made of two sensors (B and D) and 24 ASICs, 12 on each side. The outer layer detector is bigger than that for the inner layer. It is made of three sensors (A,B and C) and 32 ASICs, 16 on each side.

Sensors are ganged together strip-by-strip. ASICs are bonded only to one sensor. This is the B sensor for the inner layer detector, and the C sensor for the outer layer detector.

The Si-tracker can be operated in the minimum tracking configuration (1 inner layer and 1 outer layer) or in the extended configuration (1 inner layer and 2 outer layers).

The minimum tracking configuration was chosen as the most suitable option. This is because time and effort available for production favoured the building of the 18 detectors required in this configuration.

The tracking capability of the instrument is not necessarily improved in the extended configuration. Hits in the outermost layer are used by the tracking algorithm only if the other outer layer did not detect them. The main reason for detection inefficiencies in outer layers is the number of dead/faulty channels. Therefore the impact of the outermost layer on the tracking is negligible if layers have negligible dead area.

It is expected that the tracking performance of the minimum and extended configurations will be equivalent during the first

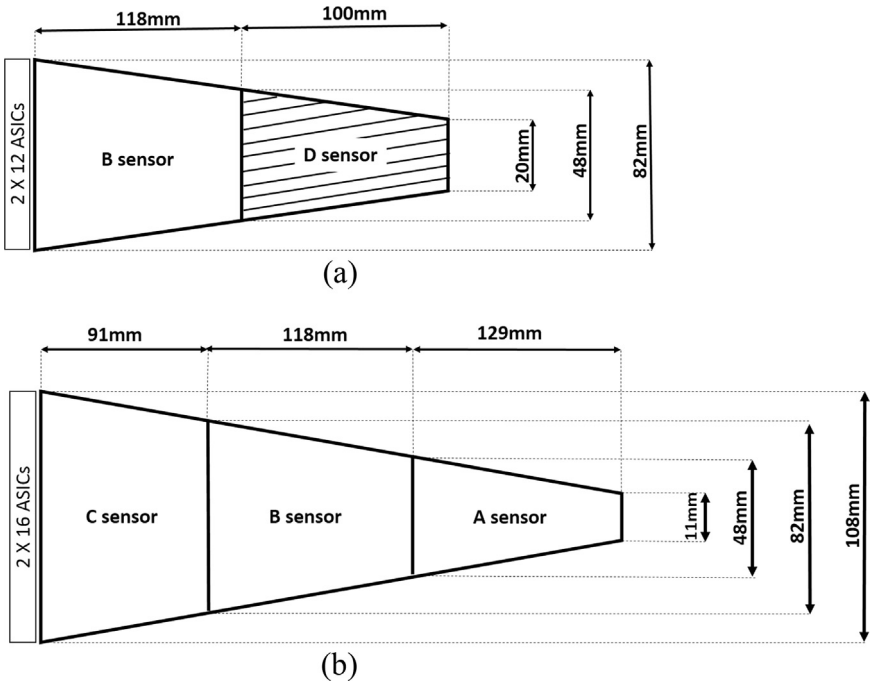

Fig. 2. Detector type for the inner (top) and outer (bottom) layers. Sensor strips have a variable length. They are parallel to one of the inclined sides of the sensor as shown on the D sensor.

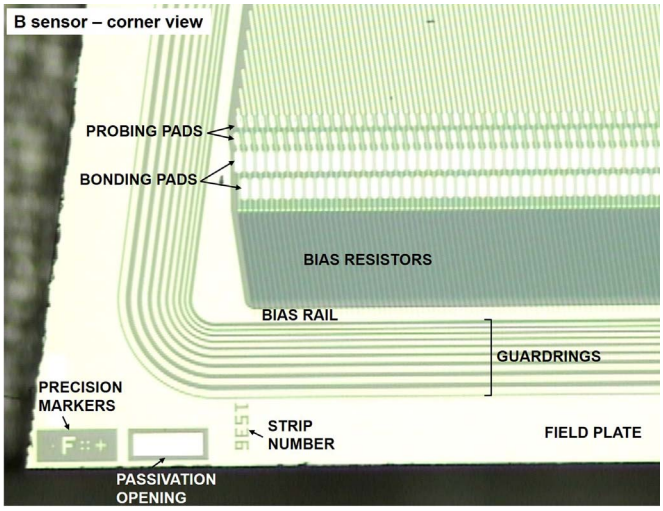

Fig. 3. Bottom-left corner of the n-side of a B sensor. The layout is identical on the n and p sides of the sensor, and for every sensor type: A,B,C,D. Key structures are outlined.

Table 1
Sensor type with corresponding active area, number of strips and measured yield. Sensors with a larger area have a lower yield.

Type	Active area (cm^2)	Strips	Yield
A	31	889	69%
B	48	1536	48%
C	49	2048	52%
D	24	876	74%

years of operation. Ageing effects on detectors possibly due to electrical stress may increase the dead area of detectors. Based on operational experience, it will be decided if it will be preferable replacing individual detectors in the minimum tracking configuration or adding the third outermost layer to the set-up.

2.1. Sensors

Sensors are produced by Micron Semiconductor Ltd [6]. The bulk growth technique is Float Zone. The bulk is n-type with high resistivity ($\sim 10^3 \Omega$ cm). The bulk thickness is 300 μm. The strip pitch is 50 μm divided in 38 μm of strip width and 12 μm of gap.

The strip length is variable. Strips are running parallel to one of the two inclined sides. Hence, they become shorter when moving from one side to the other. A sketch of this concept can be seen in the D sensor of Fig. 2. The stereo angle between the strips on the two sides is 16.2°.

N-type strips are insulated with a p-spray implant. This is to mitigate the damage produced by the TID (Total Ionizing Dose) on the silicon oxide.

The bottom-left corner of the n-side of a B-sensor is shown in Fig. 3. This is a representative area of the sensor layout. It is identical on both sides of the sensor. These devices feature nine floating guard-rings. Bias-ring and a bias resistor are also part of the sensor. They allow for a simplified procedure during quality assurance tests. In the final detector, sensors are biased directly via the pre-amplifier in the front-end electronics. Pre-amplifiers are DC coupled to the strips by wire bonding on the so-called bonding pad. Each front-end channel has a current compensation circuit capable of compensating a strip leakage current up to 100 nA. A strip is expected to have on average a leakage current of 1–2 nA.

All four type of sensors (A,B,C,D) are identical from the technology point of view. They differ in active area and number of strips as reported in Table 1.

2.2. R3B-ASIC

The ASIC [7] (Application Specific Integrated Circuit) is designed in AMS 0.35 μm CMOS technology. It provides three

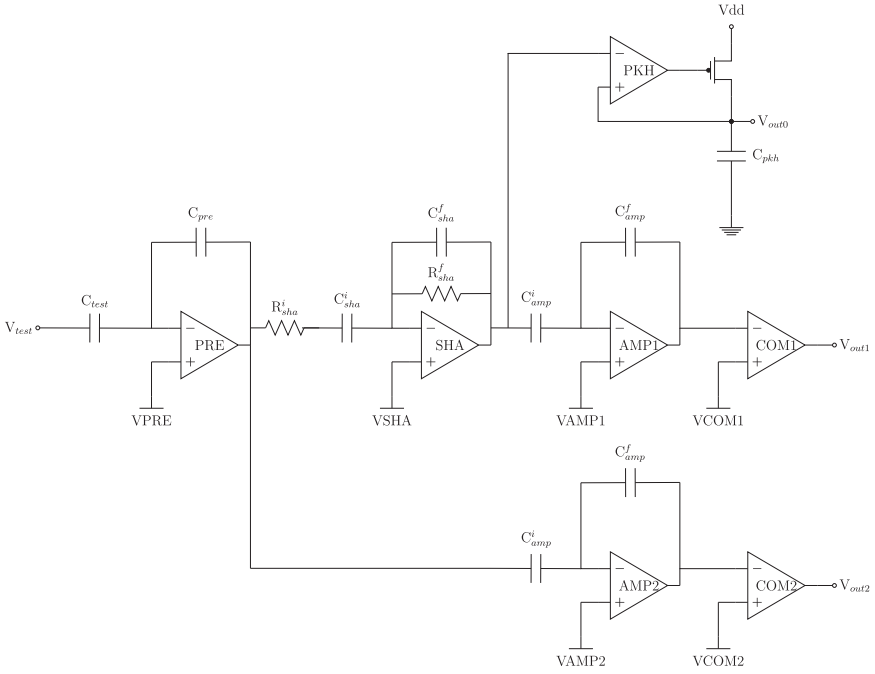

Fig. 4. The front-end channel as in the R3B ASIC. The schematic gives a simplified view of the processing stages for a positive input signal.

information: strip number, energy deposition and time of the hit. The same type of ASIC is used to condition and process signals collected on the p and n strips.

It has 128 analogue front-end channels which use a common 12 bit successive approximation ADC (Analogue to Digital Converter). The energy range of the ASIC is 40 keV–50 MeV. Schematics of the front-electronics are shown in Fig. 4.

Each channel has a charge sensitive pre-amplifier to integrate the charge induced in a strip. The signal is then filtered by a CR-RC shaper with a selectable peak-time in the range 0.5–8.0 μs and adjustable in steps of 0.5 μs. The signal is subsequently fed to a peak-hold circuit. Two comparators are present in each channel: A time-stamp comparator which generates a time-stamp from the fast rising edge of the pre-amplifier signal; and an energy comparator which validates a hit from the lower noise shaper-output.

The ASIC is capable of handling a maximum data rate of 5 kHz per channel. The maximum channel occupancy at this rate is 15% before the ASIC becomes overloaded with data.

The readout scheme is based on a daisy chain. Every fourth ASIC is grouped together. This is to keep the data rate constant in each chain. In fact, ASICs bonded to long strips have higher hit rates than ASICs bonded to short strips. Grouping adjacent ASICs together would result in an unbalanced data rate between different chains on the same detector.

3. Detector production

The goal of the detector production was to build the minimum tracking configuration. This consists of one inner layer with six detectors and one outer layer with 12 detectors. The production was performed in an ISO5 clean-room at the LSDC (Liverpool Semiconductor Detector Centre). Ten people were required to operate the production line and 7 months were necessary to complete the required 18 detectors.

Custom made equipment like jigs and tools supported detectors during production. Jigs and tools are made of anodized aluminium to increase corrosion resistance and prevent a consequent contamination of the workpiece. Flatness was an important geometrical tolerance for the design and manufacturing of tools and jigs. A flatness better than 200 μm was sufficient to guarantee a good support for the workpiece through the different stages of production. Tools for the outer layer detectors required this flatness over an area up to ~200 cm^2. Those for the inner layer detectors over an area up to ~110 cm^2.

Standard equipment was also used during construction. A smart-scope for metrology tests. A probe station to perform quality assurance on sensors. Two bonding machines to interconnect sensors and ASICs. Wire bonding was performed by using wedge-wedge ultrasonic welding with a 25 μm aluminium wire.

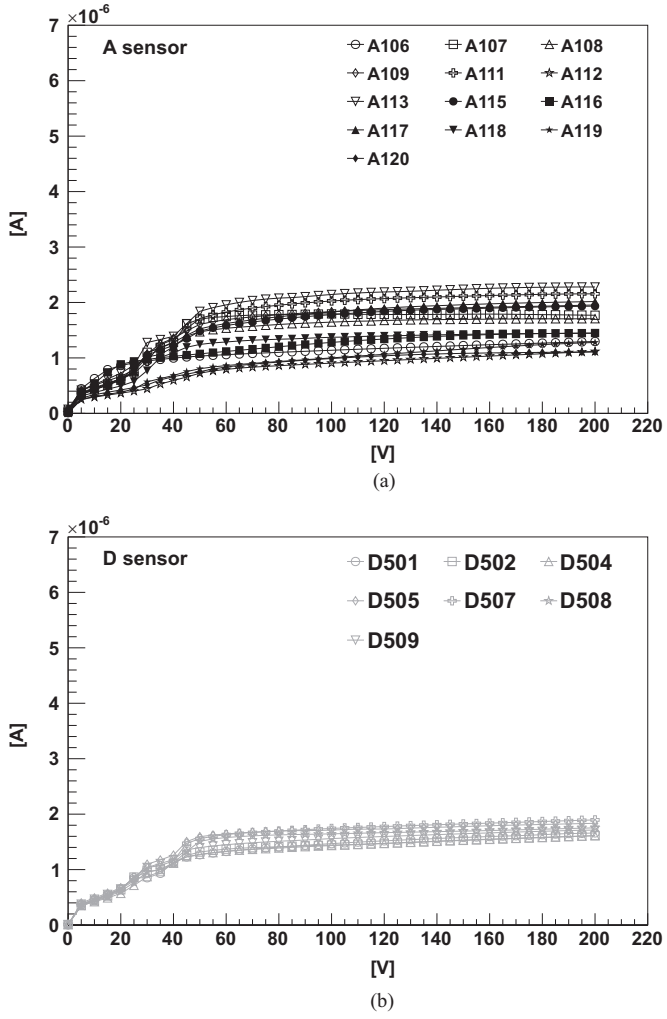

Fig. 5. *IV* curves of A and D sensors. Curves plateau at a few μA as expected. Micro-discharges appear in the region 20–40 V, but they were not considered as a criterion for sensor QA.

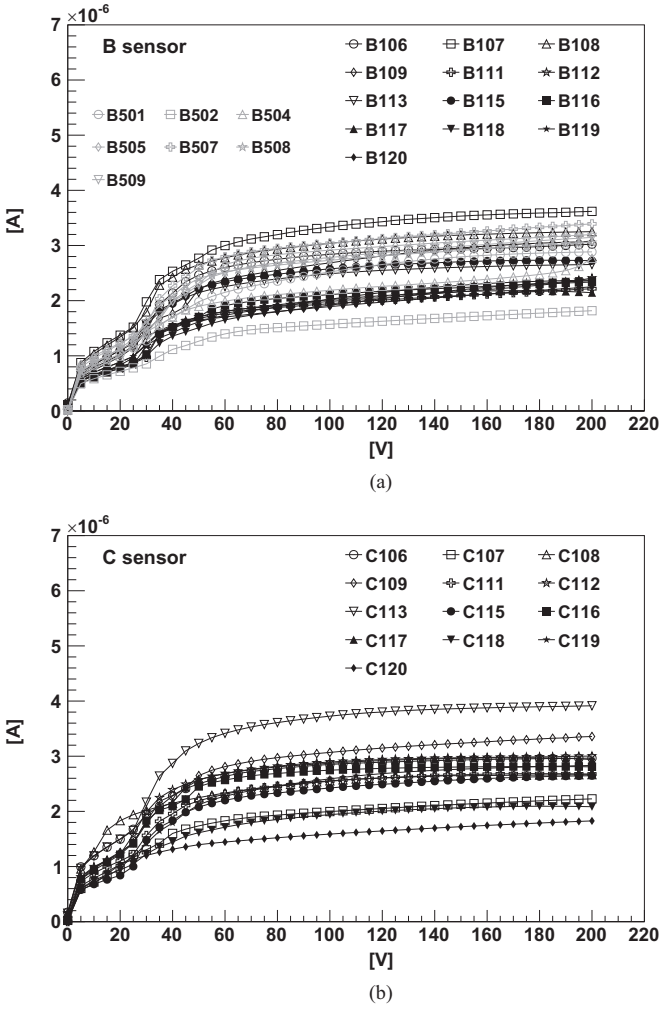

Fig. 6. *IV* curves of B and C sensors. Curves plateau at a few μA as expected. Micro-discharges appear in the region 20–40 V, but they were not considered as a criterion for sensor QA.

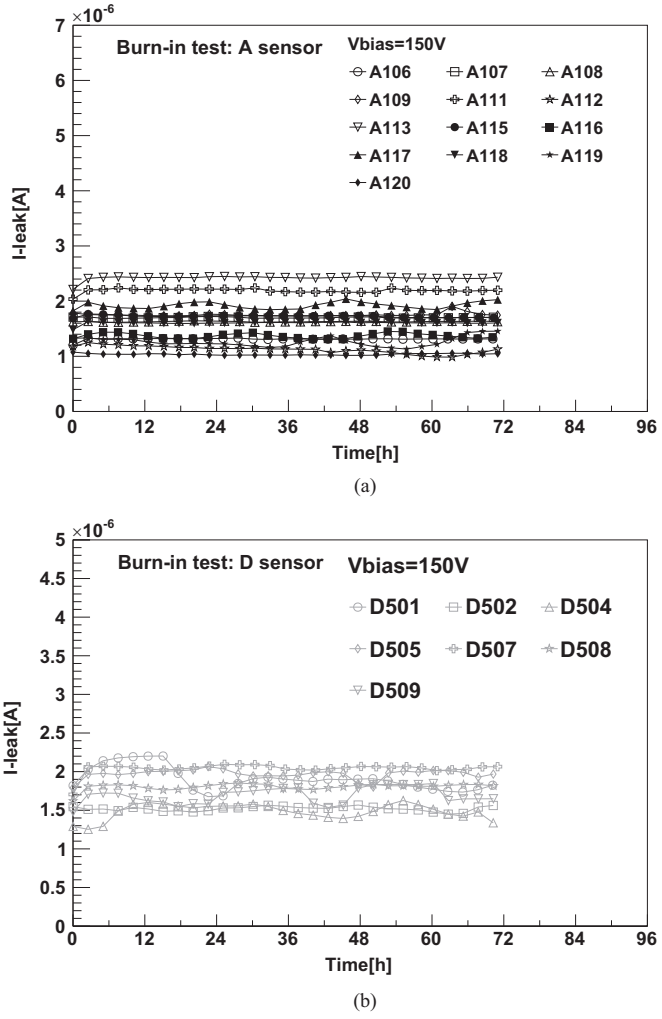

Fig. 7. Burn-in tests of A and D sensors. Sensors are biased at 150 V for 72 h. Currents are stable over time. Changes in room conditions (mainly temperature) produce ripple-like effects on the current vs. time curves.

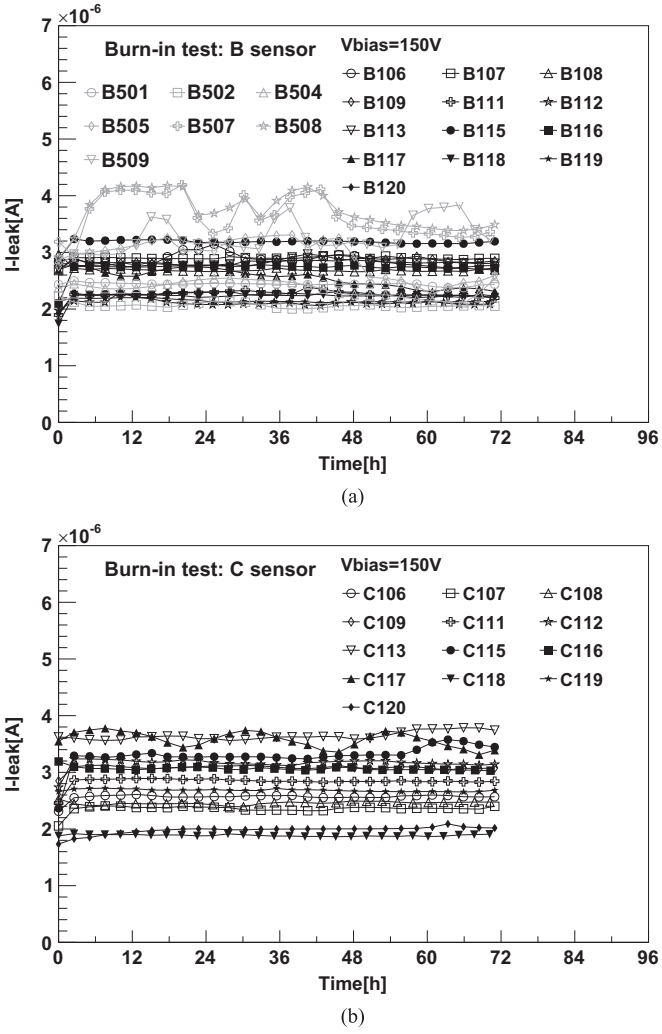

Fig. 8. Burn-in tests of B and C sensors. Sensors are biased at 150 V for 72 h. Currents are stable over time. Changes in room conditions (mainly temperature) produce ripple-like effects on the current vs. time curves. The temperature control system in the clean room experienced a fault and it was off for maintenance for some time. Sensors (e.g. B507, B508) which were tested during this period were exposed to bigger changes in temperature. The temperature in the clean-room is normally set to 21 ± 1 °C.

About 160,000 bonds were necessary to produce the 18 detectors.

A custom made data acquisition system was used to electrically test ASICs and detectors. Tests aimed at assessing the basic functionality of the digital and analogue parts of the ASICs. Digital tests included exercising the daisy chain readout; synchronizing and decoding Manchester encoded data; writing and reading registers via I2C communication.

The analogue front-end was tested by using the internal test pulser. Test pulses were injected in a sample of eight front-end channels in each ASIC. Number of entries, mean value and standard deviation of the ADC distribution were checked.

3.1. Sensor QA

Sensors were selected based on a QA (Quality Assurance) procedure. Data presented in this section refer only to those devices which are mounted on detectors which were successfully built and flagged as "pass". Sensors are named after the detector to which they are mounted on.

Sensors were visually inspected for mechanical damage (like cracks) due to wafer sawing or handling during shipment. The global electrical quality was tested by performing *IV* characteristics on the device. The sensor *IV* was measured by keeping it in darkness at room temperature and pressure. Sensors were selected by looking at the leakage current value from the curve plateau. For a good device this value should correspond to a few μA. *IV* characteristics are shown in Figs. 5 and 6. "B" and "C" sensors have similar leakage current because they have similar volumes. The smaller volume of "A" and "D" pieces results in lower values of leakage current. *IV* curves show evidence of micro-discharges, but this was not used as a criterion for the sensor QA.

Sensors underwent burn-in tests to check for their stability over time. Devices were biased at 150 V for 72 h and their leakage current monitored. All the sensors show a stable behaviour. Plots are shown in Figs. 7 and 8. Changes in leakage current are due to changes in room conditions: like temperature. The temperature in the clean-room is normally set to 21 ± 1 °C. Some sensors (e.g. B507, B508) were exposed to bigger changes in temperature. This is because the cooling system in the clean-room was switched off for maintenance during that period.

Sensors were also tested to detect local defects (like faulty strips) by probing each individual strip. They were rejected if an individual piece had more than ~5 strips with leakage current higher than ~5 times the average value: 1–2 nA.

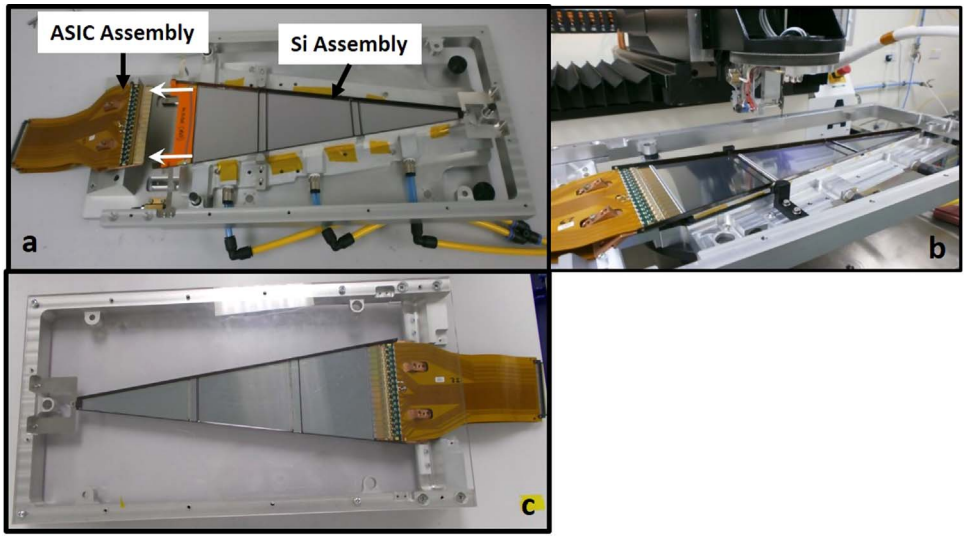

Fig. 9. Production of an outer detector: (A) ASIC-assembly and Si-assembly are jointed together; (B) bonding of FE to strip; (C) complete detector.

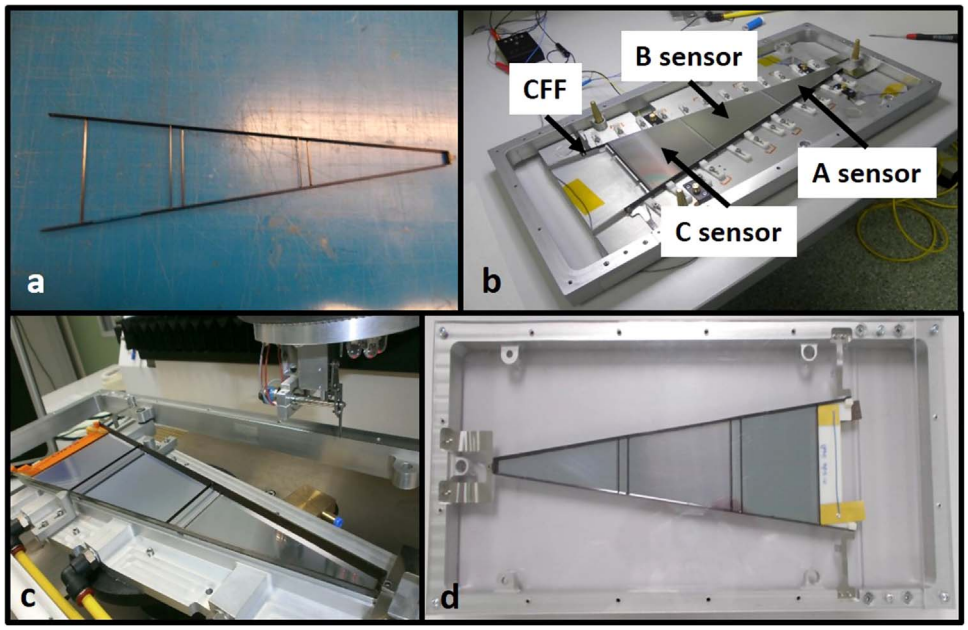

Fig. 10. Production of an outer Si-assembly: (A) Carbon Fibre Frame (CFF); (B) gluing of sensors to CFF; (C) ganging sensors; (D) complete Si-assembly.

The measured yield of each sensor type is reported in Table 1. "B" and "C" sensors have a lower yield than "A" and "D" sensors. The yield is proportional to the area of the sensor. A small-area sensor has a low probability of having a defect within itself.

3.2. Assembly procedure

A detector is made by joining together a Si-assembly and an ASIC assembly. The assembling procedure of an outer layer detector is shown in Fig. 9. A tool holds in place the ASIC assembly and permits to slide in place the Si-assembly (Fig. 9a). The two entities are attached one to the other by using a multi-purpose, two component, room temperature curing, paste adhesive of high strength and toughness: Araldite 2011®. The last step of the production is to wire-bond each strip on the sensor to its corresponding front-end channel (Fig. 9b). A picture of a complete detector is shown in Fig. 9c.

The production flow of an outer layer Si-assembly is shown in Fig. 10. It consists of silicon sensors mounted on a CFF (Carbon Fibre Frame) and ganged together. Silicon sensors are selected after performing the QA procedure described in Section 3.1.

A CFF is shown in Fig. 10a. It is made by attaching together several different bars in a trapezoidal shape. Carbon fibre bars are made by putting carbon fibres into a mould and then filling the mould with epoxy resin. CFFs are coated with a layer of insulating lacquer. The insulation of the frame is tested by measuring the resistivity of the CFF surface with a probe and a multimeter. CFFs are also metrology tested to check that the height of the cross bars are within a couple of 100's μm with respect to the long side bars. A good joint between bars ensures a good mechanical contact between sensors and CFF at the gluing stage.

Sensors are glued on the CFF (Fig. 10b) by using the same multi-

purpose paste adhesive described above. The longitudinal alignment between the sensors and the CFF is metrology tested and it is required to be <25 μm. Finally, sensors are wire bonded together (Fig. 10c) strip by strip on each side.

The key steps in the construction of an outer layer ASIC-assembly are shown in Fig. 11. An ASIC-assembly carries the ASICs providing them electrical connections and cooling. The cooling block (Fig. 11a) is made of copper and it is needed to remove the heat generated by the ASICs. It will be mechanically connected to the cooling system operating in the vacuum chamber.

Two identical FPCs (Flexible Printed Circuits) are used in an ASIC assembly (Fig. 11b). One on each side of the cooling block. FPCs are connected to cooling blocks by using a bi-adhesive copper tape. The design of the FPC in the region where the ASICs are mounted took into account two needs. The first one is maximizing the heat transfer between ASICs and cooling block. The second one is electrically insulating ASICs from the cooling block. The FPC in this region has a thickness of ~70 μm, divided into ~50 μm of kapton and ~20 μm of copper. The surface of contact with the cooling block is also maximized. Tracks and pads on the FPC are made of copper. The exposed ones are Ni–Au plated to maintain good bonding capabilities by preventing copper oxidation.

ASICs are mounted on the FPC (Fig. 11c) by using a thermally conductive glue. This is a two-component silver-filled epoxy curing at room temperature: Loctite Ablestik 2902®. A few hundred microns of glue is applied on the FPC using a stencil technique. ASICs are then positioned on top of it.

ASICs are first bonded to the FPC. This provides connection to analogue and digital bias voltages, clocks, data lines and daisy chain control signals. ASIC to ASIC bonds are also connected to transmit signals like I2C communication.

Intermediate products are electrically tested many times during construction to detect failures at early stages of production and reject or rework them.

The description of the assembly procedure focused on the construction of the outer layer detectors. An identical procedure is followed for the inner layer detectors which feature smaller components (like sensors, CFF and FPC) and less ASICs (12 per side).

3.3. Outcome

The detector production started with the outer layer. Thirteen detectors were flagged as "pass" out of the 15 built in total. This resulted in a yield of ~85%. Two detectors were rejected because of electrical problems. The first one had a broken daisy chain. The second one had an unstable leakage current which was rapidly drifting to high values (> 20 μA) over time.

The production of the inner layer followed that of the outer layer. In this case, seven detectors were flagged as "pass" out of the nine built in total. This corresponds to a yield of ~75%. Two detectors were rejected. The first one because it was mechanically damaged (crack on sensor) during handling. The second one because of high leakage current (> 20 μA).

IV curves for all the complete detectors are shown in Fig. 12. In these *IV* scans, the maximum bias voltage (80 V) was chosen to be about 50% higher than the nominal full depletion voltage (53 V). Outer layer detectors have an higher leakage current than the inner layer detectors. This is because the sensor volume is bigger in the outer layer detectors (three sensors: A,B,C) than in the inner layer detectors (two sensors: B,D).

Finally, an example of functionality tests on detectors is reported. The aim of the tests is to verify the functionality of the front-end electronics. Plots for a representative detector (outer 119) are shown in Fig. 13. They are referring to tests performed on the p-side (junction side) of the detector. In total 128 channels (8

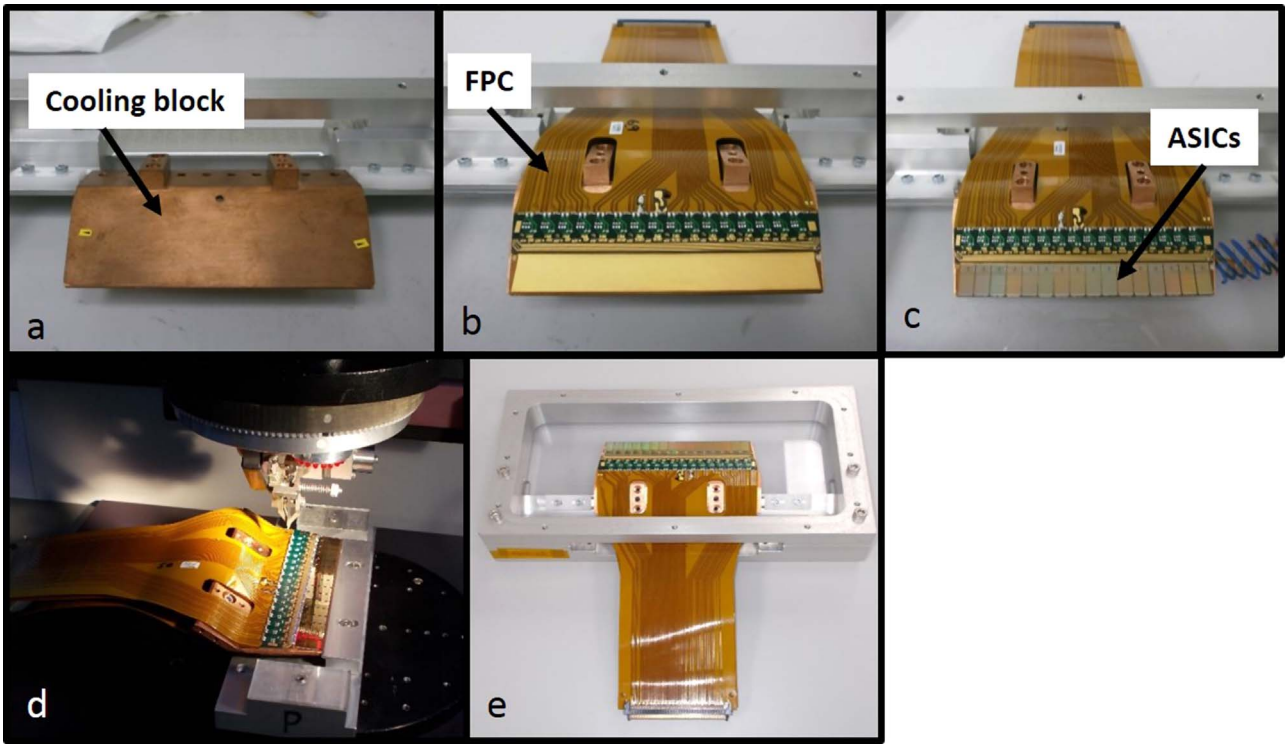

Fig. 11. Production of an outer ASIC-assembly: (A) bare cooling block; (B) FPCs mounted on cooling block; (C) ASICs populating FPCs; (D) bonding of ASICs; (E) complete ASIC-assembly.

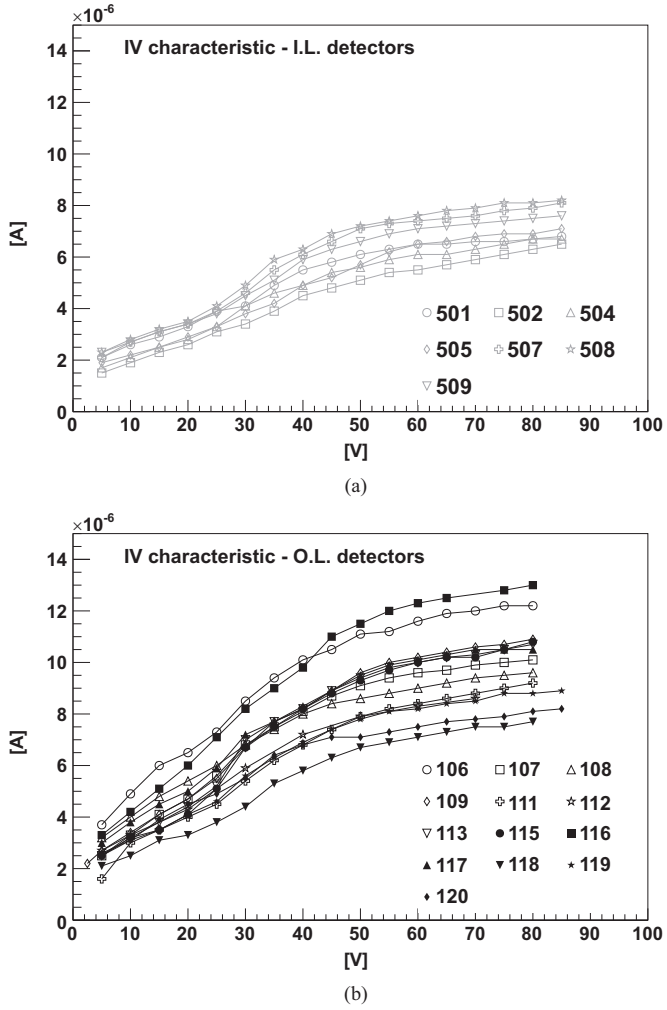

Fig. 12. *IV* curves of those detectors which were flagged as "pass" during production. Inner layer (I.L.) detectors have a lower current than outer layer (O.L.) detectors. This is because of the different sensor volume: two sensors in I.L. detectors; three sensors in O.L. detectors.

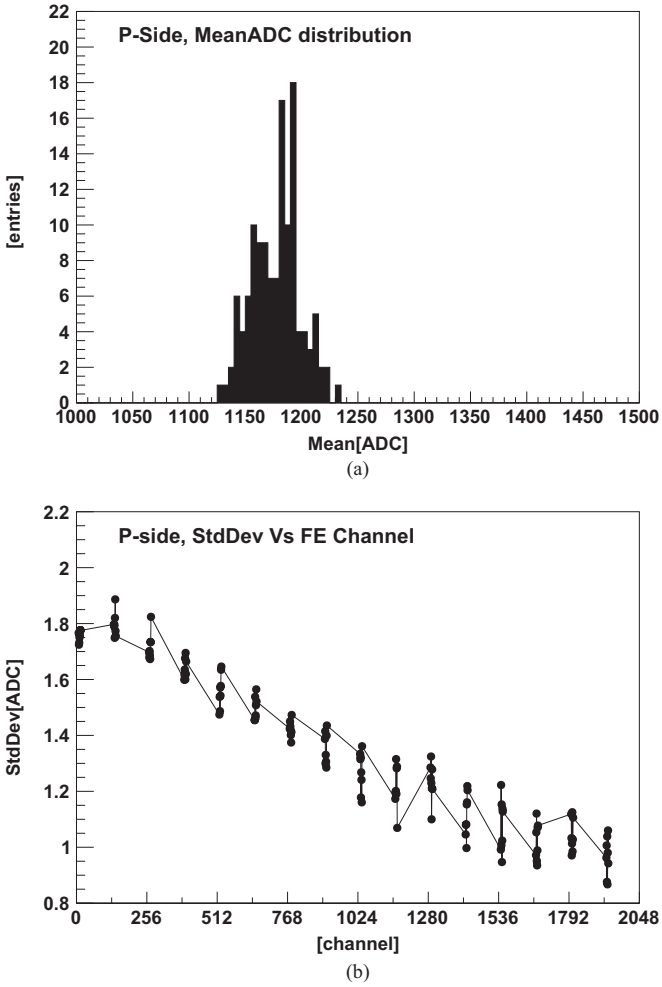

Fig. 13. Electrical tests to check the ASIC functionality: (A) Distribution of mean ADC values showing that a number of ~1200ADC is expected for an injected pulse of ~1.6 MeV. (B) Standard deviation versus front-end channel showing that the noise is proportional to the strip length: channel 0 longest strip; channel 2047 shortest strip.

per ASIC) were pulsed at the same time. The peak-time of the shaper was set to 1.5 μs. The detector was biased at 65 V. This bias voltage is the chosen operating voltage for the detectors and it is about 20% higher than the full depletion voltage (53 V).

Fig. 13a shows that for an injected pulse of ~1.6 MeV the mean value of the ADC distribution is ~1200ADC. Fig. 13b shows that the standard deviation of the ADC distribution of the channels decreases as a function of the strip length: channel 0 longest strip; channel 2047 shortest strip. This is expected because the noise is a function of the input capacitance and leakage current. Both depending on the strip length.

4. Conclusion

The R3B Si-tracker will take data at FAIR. It will be operated in the minimum tracking configuration: 1 inner and 1 outer layer. This corresponds to a total of 18 detectors: 6 inner and 12 outer detectors. The production phase delivered 7 inner and 13 outer detectors. Giving the opportunity of having one spare for each layer.

Acknowledgements

The authors would like to acknowledge STFC for funding the NUSTAR project. They would also like to thank the following people at the University of Liverpool. K. McCormick and all the mechanical workshop for adapting jigs and tools for the production. P.Cooke and P.Sinclair at the composite laboratory for making Carbon Fibre Frames. M. Wormald and L. Boynton for their assistance in wire-bonding operations. T. Jones for allocating space and equipment in the clean-room. D. Seddon for providing mechanical drawings.

References

[1] H. Gutbrod et al., FAIR Baseline Technical Report, vol.1, ISBN 3–9811298-0–6.
[2] R. Krucken, The NUSTAR facilty at FAIR, J. Phys. G Nucl. Part. Phys. 31, pp.S1807-S1811.
[3] H. Geissel, TDR on the SUPER-FRS, ⟨http://www.fair-center.eu⟩.
[4] H. Gutbrod et al., FAIR Baseline Technical Report, vol. 4, ISBN 3–9811298-0–6P, pp.41–82.
[5] ATLAS Collaboration, ATLAS Inner Detector, Technical Design Report TDR 4.
[6] Micron Semiconductor Ltd., ⟨http://www.micronsemiconductor.co.uk⟩.
[7] L. Jones, A 128-channel event driven readout ASIC for the R3B tracker, J. Instrum. 11, C02076.